IEEE Access
Multidisciplinary | Rapid Review | Open Access Journal

Received October 27, 2020, accepted November 12, 2020, date of publication November 17, 2020,
date of current version December 2, 2020.

Digital Object Identifier 10.1109/ACCESS.2020.3038381

Load Distribution Optimization of Multi-Source District Heating System Based on Fuzzy Analytic Hierarchy Process

HAORAN ZHANG[1], DONGNIAN YIN[2], XIAOJIE LIN[1,3], RONG LIU[4], WEI ZHONG[1], AND CAISHAN CAO[5]

[1]College of Energy Engineering, Zhejiang University, Hangzhou 310027, China
[2]Wuxi Huilian Thermal Power Company Ltd., Wuxi 214174, China
[3]Changzhou Industrial Technology Research Institute, Zhejiang University, Changzhou 213022, China
[4]Beijing District Heating Group Company Ltd., Beijing 100028, China
[5]Linglong Group Company Ltd., Yantai 265406, China

Corresponding author: Xiaojie Lin (xiaojie.lin@zju.edu.cn)

This work was supported in part by the National Key Research and Development Program of China under Grant 2020YFE0200400 and Grant 2017YFE0114700, in part by the National Natural Science Foundation of China under Grant 51806190, in part by the Shandong Provincial Major Science and Technology Innovation Project under Grant 2019JZZY020802, in part by the National Key Research and Development Program of China under Grant 2017YFA0700305, and in part by the Zhejiang University & Guolian Huaguang Smart Energy System Joint Research Center.

ABSTRACT As part of the energy structure transition, a key focus in district heating systems is the load distribution optimization of multiple heat sources under the specific heating network. A multi-objective optimization approach is discussed in this paper with a goal of achieving complementary advantages among heat sources, and improving the performance of the system in terms of economic cost, energy structure, and environmental benefits. This paper firstly establishes the mechanism model for multi-source district heating systems (MSDHS). Secondly, it proposes a multi-objective optimization system to account for the operation economy, energy structure, and environmental impact for MSDHS. The selected objectives are such selected that they could be justified and used in real sites. The weights of the objective functions are obtained via the fuzzy analytic hierarchy process (FAHP). Finally, this paper solves the optimization problem via particle swarm optimization (PSO) to obtain the optimal load distribution and tests its validity in a real heating system covering an area of 15 million m^2. The optimized load distribution scheme achieves a coal saving of 1.14%, a natural gas saving of 0.53%, and a cost-saving of $3,270 during a 24-hour pilot operation. This study provides the basis for future optimization enhancement and algorithm development.

INDEX TERMS District heating system, fuzzy analytical hierarchy process, load distribution.

NOMENCLATURE

ACRONYMS

AHP	analytic hierarchy process
CHP	combined heat and power
DEA	data envelopment analysis
DHS	district heating system
DOM	dynamic-objective method
FAHP	fuzzy analytic hierarchy process
IDHS	indirect district heating system
MOO	multi-objective optimization
MSDHS	multi-source district heating system
PSO	particle swarm optimization

SYMBOLS

A	fuzzy complementary judgment matrix
A^*	Complementary judgment matrix corresponding to w_{cal}
α	model parameter to be identified of the gas-fired boiler
a_{ij}	binary weight distribution of the relative importance of i and j
a_{ji}	binary weight distribution of the relative importance of j and i
β	environment pollution value
C	basic loop vector of the heating network
C_0	fuel price, \$/t or \$/m^3

The associate editor coordinating the review of this manuscript and approving it for publication was Qiuye Sun.

c_1, c_2	acceleration factor
D	mass flow rate of the working fluid, t/h
D_0	overall heat load of the system
D_k	heat load provided by the *k-th* heat source
E	section vector of the heating network
E_k	power generation of heat source k in dispatching period, MW
$F(x)$	objective function of a multi-objective optimization problem
P_L	power transmission loss
P_k	power provided by the *k-th* heat source
$P_{e,k}$	on-grid price, \$/kWh
$P_{h,k}$	heating profit, \$/t
ΔP	pressure drop vector of sections
p_{ij}	admissible deviation of the judgment matrix
p'_{ij}	random variable with zero mean
Q	heat absorption of the equipment, kW
q	net mass flow rate vector of the nodes
T	maximum number of iterations
ΔT	dispatch period, h
V	node vector of the heating network
$v_{\max}$	maximum particle speed
$v_{ij}(t)$	j-dimension flight speed of the particle i when it evolves to the *t-th* generation
$V_i =$ $(v_{i1}, v_{i2}, \ldots, v_{in})$	current flying speed of particle i
W	work of the equipment, kW
w	weight
Δw_i	deviation between the working fluid flow rate and the specified flow rate in a section
$x_{ij}(t)$	j-dimensional vector of particle i when it evolves to the *t-th* generation
X	association matrix of nodes and sections
$X_i =$ $(x_{i1}, x_{i2}, \ldots, x_{in})$	current position of particle i
χ	ratio of pollutants emitted from fuel combustion
Y	association matrix of sections and basic loops
η	equipment efficiency
δ	boolean state variable signifying whether the heat source supplies power
δ_{wi}	the maximum allowable deviation
ε	arbitrarily small positive number
λ_w	penalty coefficient for flow rate deviation in heat supply quality calculation
Ψ	maximum load increasing rate

SUBSCRIPT

f_w	velocity deviation coefficient of the pipe network
$g_l(x)$	expression of a constraint
$gbest(t)$	best position that all particles have experienced
$G(D)$	utility function
h	enthalpy of the working fluid, kJ/kg
Δh	enthalpy change of the working fluid, kJ/kg
K	number of heat sources
LHV_f	low heating value of the fuel, kJ/kg
M_f	mass flow rate of the fuel, kg/h
N	population size
$ncmp$	number of the working fluids in a device module in the CHP system
P_0	overall power demand of the system
ac	amount of constraints
b	boiler
cal	calculated
cmp	component
f	fuel
fw	boiler feed water
g	sequence number of gas-fired boiler heat sources
k	sequence number of heat sources
ms	main stream
rh	reheat steam
ri	reheat steam inlet
ro	reheat steam outlet

I. INTRODUCTION

A. BACKGROUND

In 2010, nearly 70% of China's urban area's heat demand was supplied by small coal-fired boilers [1]. Due to the rapid increase in the building area (from 2001 to 2016, the area of cities and towns in northern China increased from five billion m^2 to 13 billion m^2) [2], clean heating has become a centerpiece in China's emission control policy. That leads to a dramatica change of district heating source structure. The ongoing trend is the shift from small coal-fired boilers to combined heat and power (CHP) units as the main source and peaking boilers as a supplement. As of 2017, more than 50% of the heat demand for urban district heating in China was provided by CHP units, and the coal consumption of heating in North China was 5.8 billion GJ [3]. Such change of heating source structure in China is part of the continuous renovation of urban energy systems.

The foundation of the multi-source district heating systems (MSDHS) optimization is building its mechanism model, which provides data support for the optimization process. A lot of researchers have made their contributions to the modeling of MSDHS [4]–[6]. Yang *et al.* separated the district heating system (DHS) into three major parts: the straight pipe, four kinds of local pipes, and the radiator [7]. Their work built a steady-state model of the DHS that included hydraulic and thermal sub-models. Li *et al.* implemented both steady-state modeling and dynamic modeling of the indirect district heating system (IDHS) [8]. Respectively, the steady-state model was used to study the impact of important

system parameters, and the dynamic model based on energy balance was used for the efficiency analysis of the system. Unlike the above studies, Choi *et al.* considered the thermal power plant as the core component of the district heating system, and the validation of the model was verified by the case study [9].

Based on modeling, researchers who have a special interest in the field of MSDHS optimization could focus on the single-objective optimization of the system. From the perspective of improving economic performance, Karlsson *et al.* studied the economic potential of multiple heating operators for regional combined heating [10]. Similarly, Zhang conducted an economic analysis of heat load distribution in MSDHS through hydraulic calculation [11]. His objectives were the optimized design of the heating network and the scheduling of multiple heat sources. Similarly, regarding the optimal scheduling of heating systems, Bowitz and Trong applied the cost-benefit analysis method on the system economic performance optimization [12].

In recent years, due to the vigorous promotion of sustainable development, researchers have shifted their focus on the MSDHS optimization field from conventional single-objective optimization to multi-objective optimization (MOO), including economy and environmental protection. Xu *et al.* quantitatively analyzed the economic and environmental advantages of Canada's MSDHS using an energy balance model [13]. Agrell and Bogetoft used the Data Envelopment Analysis (DEA) method to comprehensively evaluate the economic and environmental benefits of the Danish district heating system driven by CHP units [14]. Hamalainen and Juha proposed a dynamic multi-indicator optimization model for heating systems considering load fluctuation conditions [15]. Their work included a case study with the goal of heating energy consumption, heating cost, and temperature range. Incorporating more goals into their study, Zheng and Cai analyzed and compared different heating modes from three aspects of the economy, environmental protection, and technology [16]. Their work adopted the gray system multi-objective comprehensive effect measurement method to choose the better heating mode. Besides, based on fuzzy mathematics, Liu and Ang established a multi-level mathematical model for the comprehensive optimization of heating systems [17]. Zhang and Ding denoted the uncertainty factors in the central heating system with vectors to simplify the optimization process [18]. Li *et al.* proposed a two-stage method that combines multi-objective optimization (MOO) with integrated decision making (IDM) to address the problem of combined heat and power economic emission dispatch [49].

From existing studies, it should also be noted that the integration of objectives through the weight method is widely used since it can reduce the decision-making cost. The key is the selection of the weights. Weight methods rely on the data source and can be divided into two types: objective methods and subjective methods. Common objective weighting methods include the entropy weight method, principal component analysis, and fuzzy comprehensive evaluation. Among them, the entropy method is widely used in indicator analysis and risk assessment [19]–[21]. The analytic hierarchy process (AHP), first proposed by Saaty *et al.* [22], is a representative subjective weight method. It combines quantitative analysis with qualitative analysis and uses the experience of decision-makers to judge the relative importance of each indicator. Researchers have made improvements to the original AHP method and proposed new methods such as improved AHP, fuzzy AHP, extension fuzzy AHP, and grey AHP [23].

As for the optimization algorithm selection, particle swarm optimization (PSO) has been widely used in the multi-objective optimization (MOO) field [24], [25]. It is a global search algorithm first proposed by Eberhart and Kenedy in 1995 [26]. It simulates the migration and gathering behavior of birds in the process of foraging and uses the intelligence of the group to search for better solutions. However, the traditional PSO has a poor local search capability, and the search performance is dependent on parameters. Therefore, researchers have proposed improved methods of PSO. In terms of parameter setting, Chatterjee *et al.* proposed a PSO algorithm with non-linear changes in inertia weight [27]. Ratnaweera *et al.* proposed an asynchronous time-varying acceleration factor [28]. At the same time, researchers have analyzed the convergence of the algorithm and proposed methods to improve the convergence [29]–[31]. A large number of engineering practices show that compared with other optimization algorithms, particle swarm optimization needs fewer parameters to adjust, and its structure is simple, so it is easier to implement in engineering.

Overall, when compared with conventional district heating systems, well-operated multi-source district heating systems (MSDHS) are expected to achieve the following advantages. First, it can safeguard the use of heat sources with volatility and instability, which are driven by renewable energy. Second, it can ensure good performance on the economy, environmental protection, supply reliability, and scheduling flexibility of the urban heating system. Third, it can achieve coordinated operation of renewable energy, industrial waste heat, cogeneration, and regional boilers (if necessary) under the circumstances that the scale of urban heating is expanding. The specific implementation method of MSDHS is applying real-time optimization of multi objectives such as economy, energy structure, and environment to load distribution among heat sources so that the merits of complementary advantages can be fully realized.

However, such the expected effect of emission reduction has not been achieved so far in China's large-scale MSDHS due to the fact that MSDHS still follows the conventionally empirical and even manual operation control formulated for single-source small-scale heating systems. The key problem is that there is no practical multi-constraint and multi-objective heat load distribution method in China's MSDHS that considers the diversity of the current heating source structure.However, the heat load distribution of the MSDHS is critical to its operation benefits. For example,

when the heat demand is low, the system should utilize heat sources with higher efficiency or are more environmentally friendly. However, when the heat demand is high, the first priority is to operate the heat sources connected to the grid complementarily. Such a tradeoff between operation economy and environmental impact is necessary. Moreover, even with the same type of heat sources, the efficiencies of the sources are impacted by fuel type, model number, and load conditions. For example, the CHP units and boilers have a peak in their performance curves, as shown in Fig. 1 and Fig. 2 [32], [33]. In MSDHS, it is critical to find a reasonable load distribution ensuring that each heat source (boiler and CHP units) is in an efficient working condition during the dispatching period.

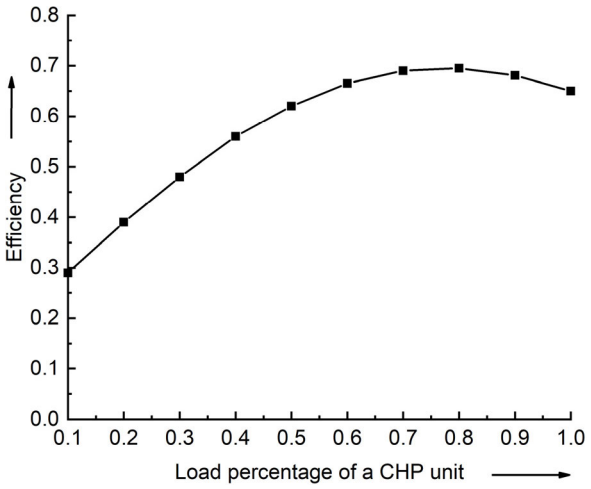

FIGURE 1. The efficiency of a CHP unit under different load conditions.

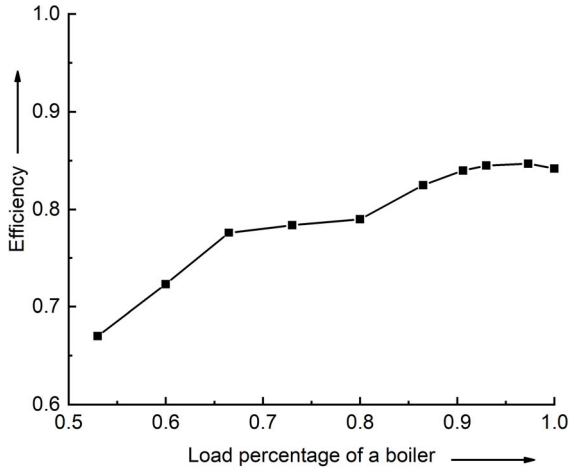

FIGURE 2. The efficiency of a boiler under different load conditions.

Moreover, researches have not been seen that consider the multi-source load distribution strategy of the heating system under the constraints of the operation of the heating network and comprehensively optimize the economy, energy structure, and environment. Along with the transition of urban heating systems, a major trend in this area is to take into account the demand aspect from the heating network with a complex topology structure during the operation of MSDHS, such as what Cai *et al.* mentioned in the heating system demand-side management study [34].

B. MOTIVATION

Overall, the existing studies haven't discussed the critical issue of load distribution problem in MSDHS. As discussed above, such load distribution should be taken care of under the general framework of MOO discussed in the previous studies taking into account the economic and environmental requirements and coal substitution. In addition, this study investigates the optimization of multi-source load distribution by considering both the heating network and the source coordination and introducing network transport capability constraints. The goal is the validate the approach of MOO in both simulation and on-site tests to verify the feasibility of optimized dispatching strategies in real MSDHS.

The rest of the paper is organized as follows: Section II illustrates the structure of a typical MSDHS and sets up the mechanism model for MSDHS, including its sources and network. Section III establishes an indicator system for MSDHS based on the fuzzy analytic hierarchy process (FAHP) and proposes a multi-objective optimization model for load scheduling and its solving method. Section IV and section V discuss the results when the proposed methodology is applied to a real heating system in Beijing and conclude with the findings from the study, respectively.

II. MODELING OF MSDHS

Referring to the current situation of China's urban heating systems [35], the heat sources of the MSDHS considered in this paper are mainly composed of CHP units and gas-fired boilers (peaking boilers). Moreover, the modularity and identification modeling methods described below also apply to the construction of a general model of MSDHS that contains renewable energy and industrial waste heat. This paper firstly constructs an MSDHS model to solve the corresponding relationship between fuel quantity and heat load. Besides, the heat supply for the load side in the model is obtained by prediction.

A. CHP UNITS

Based on the modular modeling method, this paper simulates the full working condition characteristics of a CHP unit under a steady state. Any device module in the CHP system can be modeled using the following equation:

$$\eta \sum_{cmp=1}^{ncmp} D_{cmp} \Delta h_{cmp} - Q - W = 0 \tag{1}$$

where η is the equipment efficiency. $ncmp$ is the number of working fluids in a device module in the CHP system. The subscript cmp represents the cmp-th working fluid. D is the mass flow rate of the working fluid, t/h. Δh is the enthalpy change of the working fluid, kJ/kg. Q is the heat absorption of the equipment, kW. W is the work of the equipment, kW.

As an illustrative example, the boiler module's energy balance equation is as follows:

$$D_0\left(h_{ms}-h_{fw}\right)+D_{rh}\left(h_{ro}-h_{ri}\right)=Q_b \tag{2}$$

where D_0 is the overall heat load of the system. h_{ms} is the enthalpy of the mainstream. h_{fw} is the enthalpy of the boiler feedwater. D_{rh} is the mass flow rate of the reheat steam. h_{ro} is the enthalpy of the reheat steam outlet. h_{ri} is the enthalpy of the reheat steam inlet. Q_b is the heat absorption of the boiler, kW.

The first item in the above formula is the heat input from fuel-burning:

$$D_0\left(h_{ms}-h_{fw}\right)=M_f LHV_f \tag{3}$$

where M_f is the mass flow rate of the fuel, kg/h. LHV_f is the low heating value of the fuel, kJ/kg.

B. GAS-FIRED BOILERS

During operation, natural gas and electricity consumption of gas-fired boilers are key considerations as they constitute the major sources of pollution [36]. For simplicity, this paper uses the identification method to build the gas boiler model, and only considers the influence of the boiler's heat load on its thermal efficiency. Therefore, the performance curve of the d th gas boiler, which illustrates the relationship between the heat load D and the fuel consumption f, can be obtained by using the least square method:

$$f_d\left(D_d\right)=\alpha_{d0}+\alpha_{d1}D_d+\cdots+\alpha_{dc}D_d^c \tag{4}$$

where α is the model parameter to be identified of the gas-fired boiler.

In this paper, (4) takes the quadratic polynomial to meet the accuracy requirements.

C. HEATING NETWORK

In this paper, a graph-based method is used to establish a mathematical model describing the topology of the heating network, and the solution of the network balance is solved by Kirchhoff's law. The specific process is as follows:

1) The heating network topology is described as a directed flow chart containing M nodes (heat sources, users, pumps, etc.), N sections (pipes), and S basic loops. These components are represented by vectors, respectively:

$$V=\{V_1,\ldots,V_m,\ldots,V_M\}\quad(1\le m\le M) \tag{5}$$
$$E=\{E_1,\ldots,E_n,\ldots,E_N\}\quad(1\le n\le N) \tag{6}$$
$$C=\{C_1,\ldots,C_s,\ldots,C_S\}\quad(1\le s\le S) \tag{7}$$

where V is the node vector of the heating network. E is the section vector of the heating network. C is the basic loop vector of the heating network.

2) The association matrix X $(M\times N)$ is used to represent the connection relationship between any node V_m and any section E_n of the heating network. The matrix row number corresponds to the node number, and the column number corresponds to the section number:

$$X=\begin{pmatrix} X_{11} & \cdots & X_{1n} & \cdots & X_{1N}\\ \vdots & \ddots & \vdots & \ddots & \vdots\\ X_{m1} & \cdots & X_{mn} & \cdots & X_{mN}\\ \vdots & \ddots & \vdots & \ddots & \vdots\\ X_{M1} & \cdots & X_{Mn} & \cdots & X_{MN}\end{pmatrix} \tag{8}$$

The matrix element X_{mn} is defined as follows:

$$X_{mn}=\begin{cases}1 & \text{If the working fluid in section } n \text{ flows to node } m\\ -1 & \text{If the working fluid in section } n \text{ flows to node } m\\ 0 & \text{If section } n \text{ is not connected to node } m\end{cases} \tag{9}$$

The association matrix Y $(S\times N)$ is used to represent the affiliation between any section E_n and any basic loop C_S of the heating network. The matrix row number corresponds to the basic loop number, and the column number corresponds to the section number:

$$Y=\begin{pmatrix} Y_{11} & \cdots & Y_{1n} & \cdots & Y_{1N}\\ \vdots & \ddots & \vdots & \ddots & \vdots\\ Y_{s1} & \cdots & Y_{sn} & \cdots & Y_{sN}\\ \vdots & \ddots & \vdots & \ddots & \vdots\\ Y_{S1} & \cdots & Y_{Sn} & \cdots & Y_{SN}\end{pmatrix} \tag{10}$$

The matrix element Y_{sn} is defined as follows:

$$Y_{sn}=\begin{cases}1 & \text{If segment } n \text{ belongs to loop } s \text{ and is clockwise}\\ -1 & \text{If segment } n \text{ belongs to loop } s \text{ and is counterclockwise}\\ 0 & \text{If segment } n \text{ does not belong to loop } s\end{cases} \tag{11}$$

3) The node energy conservation and basic loop momentum conservation equations are established as follows:

$$XQ_{net}^T=q \tag{12}$$
$$Y\Delta P^T=0 \tag{13}$$

where Q_{net}^T is the heat absorption of heating network when working fluid temperature is T, kW. q is the net mass flow rate vector of the nodes. ΔP^T is the pressure drop vector of sections when working fluid temperature is T.

Based on (12) and (13), this paper initializes the distribution of the mass flow rate for each section based on the least square method. Then this paper uses the maximum closure difference method to redistribute the flow rate. Finally, the pressure distribution of the whole network model is solved via iterations. The detailed solving process could be found out in the authors' previous study, where an industrial heating network was used as an example [37].

TABLE 1. Binary scale values of the complementary judgment matrix.

Implication	a_{ij}	a_{ji}
i is as important as j	0.5	0.5
i is slightly important than j	0.6	0.4
i is obviously more important than j	0.7	0.3
i is strongly more important than j	0.8	0.2
i is extremely more important than j	0.9	0.1

III. MULTI-OBJECTIVE OPTIMIZATION OF MSDHS

The MOO problem refers to minimizing of several objectives simultaneously under a set of constraint conditions. The MOO problem containing *num* objectives and *ac* constrictions can be described as the following general form:

$$\begin{aligned} &\min F(x) = \min\left[f_1(x), f_2(x), \ldots, f_{num}(x)\right] \\ &s.t.\ g_l(x) \le 0, \quad l = 1, 2, \ldots, ac \end{aligned} \tag{14}$$

One of the approaches to solving the MOO problem is the weight method [38]. Due to its simplicity and engineering applicability, this paper uses weight analysis in both modeling and field tests. Through assigning weights to each objective, the objective functions are combined into a single composite function to obtain an optimal solution. However, it should be emphasized that the difficulty lies in how to determine the weights.

A. MULTI-OBJECTIVE WEIGHT ANALYSIS

According to the principle of constructing the MOO indices [39] and recent developments of MSDHS in China, this article establishes a MOO index system by referring to related researches [40]–[42]. After applying the analysis of laddered coherence, the system (consisting of the goal layer, index layer, and scheme layer) is illustrated in Fig. 3.

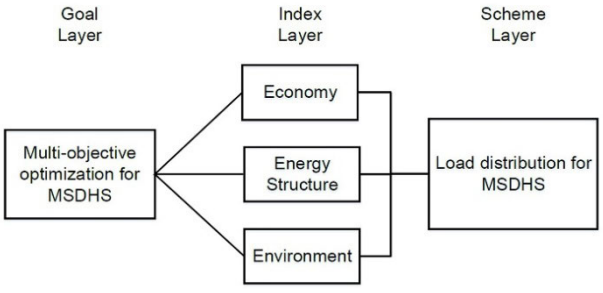

FIGURE 3. Multi-objective optimization index system for multi-heat source heating system.

In this paper, weights corresponding to the economy, energy structure, and environment on the index layer relative to the goal layer are calculated employing FAHP. The AHP has been widely used in the integrated optimization of heating systems. FAHP based on the complementary judgment matrix is one of the improved AHPs in terms of weight determination [43], [44]. The overall calculating process of FAHP in this paper can be briefly stated as following steps:

- *Step1*: Determine the binary weights according to the definitions in Table 1, and construct a fuzzy complementary judgment matrix by pairwise comparison between optimization indices.
- *Step2*: Conduct a consistency check for the matrix constructed in Step 1.
- *Step3*: Solve the judgment matrix that meets the consistency requirements to obtain the weight vector of optimization indices.

According to Table 1, fuzzy complementary judgment matrix A can be written as:

$$A = \begin{pmatrix} a_{11} & a_{12} & \cdots & a_{1n} \\ a_{21} & a_{22} & \cdots & a_{2n} \\ \vdots & \vdots & \ddots & \vdots \\ a_{n1} & a_{n2} & \cdots & a_{nn} \end{pmatrix}$$
$$\forall i, j = 1, 2, \ldots, n, 0 \le a_{ij} \le 1, a_{ij} + a_{ji} = 1 \tag{15}$$

where a_{ij} is the binary weight distribution of the relative importance of i and j. a_{ji} is the binary weight distribution of the relative importance of j and i.

Let the *i-th* and the *j-th* index be respectively w_i and w_j. Then a_{ij} is given by:

$$a_{ij} = \frac{w_i}{w_i + w_j} \tag{16}$$

where w is the hypothesis index of complementary judgment matrix, weight vector.

For fuzzy complementary judgment matrix $A = (a_{ij})_{n\times n}$, $\forall i, j, k = 1, 2, \ldots, n$, if:

$$a_{ik}a_{kj}a_{ji} = a_{ij}a_{jk}a_{ki} \tag{17}$$

Then A is said to be complementary and consistent.

If fuzzy complementary judgment matrix $A = (a_{ij})_{n\times n}$, $\forall i, j = 1, 2, \ldots, n$ does not satisfy the consistency, but

$$A' = \left(a'_{ij}\right)_{n\times m} \quad a'_{ij} = a_{ij} \pm p_{ij}, \quad \forall i, j = 1, 2, \ldots, n \tag{18}$$

satisfies the consistency, A is said to be with satisfying consistency. p_{ij} is the admissible deviation of the judgment matrix.

Assuming that deviation of judgment matrix elements is p'_{ij}, then the matrix composed by p'_{ij} is called the deviation matrix of the judgment matrix A.

$$p'_{ij} = a_{ij} - \frac{w_i}{w_i + w_j} \tag{19}$$

According to (18), the deviation optimum objective function is defined as:

$$\begin{aligned} \min \Omega &= \sum_{i=1}^{n}\sum_{j=1}^{n}\left[\left(w_i + w_j\right)p'_{ij}\right]^2 \\ &= \sum_{i=1}^{n}\sum_{j=1}^{n}\left(a_{ij}w_i + a_{ij}w_j - w_i\right)^2 \\ s.t.\ w_i &< 0, \quad \text{and} \sum_{i=1}^{n} w_i = 1 \quad i, j = 1, 2, \ldots, n \end{aligned} \tag{20}$$

where w_i is obtained by the Lagrange multiplier rule.

The judgment matrix A^* with complementary and consistency can be constructed making use of w_i, which is based on (15). After that, a consistency check is carried out through statistical hypothesis testing of the difference between matrix elements in A and A^*.

In accordance with the idea of weight determination, what this paper adopts in practice is the following three steps:

- *Step1*: Construct a fuzzy complementary judgment matrix according to the needs of different projects or stage requirements.
- *Step2*: Through the Lagrange multiplier rule mentioned above, seek a weight vector which is mostly close to the fuzzy complementary judgment matrix (optimizing (19)).
- *Step3*: According to the optimal results, weights of three indices in this paper are determined as follow:

$$w_{cal} = (0.4771, 0.2071, 0.3158) \tag{21}$$

where the subscript *cal* is the calculation result.

Complementary judgment matrix A^* corresponding to w_{cal} is presented below:

$$A^* = \begin{pmatrix} 0.500 & 0.697 & 0.602 \\ 0.303 & 0.500 & 0.396 \\ 0.398 & 0.604 & 0.500 \end{pmatrix} \tag{22}$$

B. OPTIMIZATION FORMULATION

1) OBJECTIVE FUNCTION

Based on the heating system model (used for generating system energy consumption under different working conditions) and weight vector with respect to optimization indices (applied to weight method analysis), this article specifically focuses on the MOO problem of MSDHS. At the given temperature of the working fluid, heat load distribution can be converted to mass flow rate distribution of the working fluid. The optimization functions corresponding to each index have the following forms:

Economic objective:

$$F_1(D) = \sum_{k=1}^{K} \Delta T \left[\delta_k E_k P_{e,k} + D_k P_{h,k} - f_k(D_k)\, Co_k\right] \tag{23}$$

Energy structure objective:

$$F_2(D) = \sum_{g=1}^{G} f_g(D_g) \Big/ \sum_{k=1}^{K} f_k(D_k) \tag{24}$$

Environmental objective:

$$F_3(D) = -\sum_{k=1}^{K} T\left(\beta_{SO_2,k}\chi_{SO_2,k} + \beta_{NO_X,k}\chi_{NO_X,k}\right) f_k(D_k) \tag{25}$$

where $F(x)$ is the objective function of a multi-objective optimization problem. ΔT is the dispatch period, h. δ_k is the boolean state variable signifying whether the heat source supplies power. When the heat source is a CHP unit, δ_k is a positive value, but considering the auxiliary power, δ_k is less than 1. When the heat source is a gas-fired boiler, δ_k is equal to -1. The subscript k is the sequence number of heat sources. E_k is the power generation of heat source k in dispatching period, MW. $P_{e,k}$ is the on-grid price, \$/kWh. $P_{h,k}$ is the heating profit, \$/t. Co is the fuel price, \$/t or \$/m^3. The subscript g is the sequence number of gas-fired boiler heat sources. χ is the ratio of pollutants emitted from fuel combustion.

TABLE 2. Amount of pollutants produced by fuel combustion.

Pollutant	Coal (kg/t)	Gas (g/m^3)
NO_X	9	0.63
SO_2	17s[a)]	0.1

S[a)] is the sulfur percentage of the coal.

Environmental pollution values $\beta_{SO_2,k}$ and $\beta_{NO_X,k}$ are illustrated in Table 2 [45].

Subsequently, through normalizing objective functions, the MOO utility function of MSDHS can be written as:

$$\max G(D) = \max \sum_{i=1}^{3} w_i \bar{F}_i(D) \tag{26}$$

where $\bar{F}_i(D)$ is the index performance value of the *i-th* index after normalization.

2) CONSTRAINTS

1) The constraint of heat load equilibrium and power demand equilibrium:

$$\begin{aligned} \sum_{k=1}^{K} D_k &= D_0 + D_L \\ \sum_{k=1}^{K} P_k &= P_0 + P_L \end{aligned} \tag{27}$$

2) The constraint of heat load variation range:

$$D_k^{\min} \le D_k \le D_k^{\max} \tag{28}$$

3) The constraint of increasing load rate and decreasing load rate:

$$\frac{\left|D_{k,T+1} - D_{k,T}\right|}{\Delta T} \le \Psi_k \tag{29}$$

where D_0 is the overall heat load of the system. D_L is the heat transmission loss. D_k is the heat load provided by the *k-th* heat source. P_0 is the overall power demand of the system. P_L is the power transmission loss. P_k is the power provided by the *k-th* heat source. The superscripts min and max represent the minimum and maximum heat load that the heat source can provide, respectively. $D_k^{\max}$ depends on the design capacity of the heat source. $D_k^{\min}$ refers to the lowest heat load that the heat source can provide when it can operate continuously, safely, and stably. The minimum allowable load of the boiler in a thermal power plant is generally 60%-70% of the rated load and the minimum load can reach 40-50%. ΔT is the dispatch period. Ψ_k is the maximum heating load rise and fall rate that the kth heat source can bear. For a steam turbine, too fast lifting

and lowering load rate will lead to a large temperature difference between the upper and lower surfaces of the steam turbine cylinder and the inner and outer surface, and the thermal stress of the steam turbine is too large. Therefore, the load-lifting and lowering rate of the large and medium-sized steam turbine should be controlled within 1%/min-1.5%/min to ensure the safety of the unit.

4) The constraint of transmission and distribution capacity of the heating network:

$$f_w \leq f_{w,\max} \tag{30}$$

$$\Delta w_i \leq \delta_{wi} \tag{31}$$

$$f_w = \sum \Delta w_i \tag{32}$$

$$\Delta w_i = \begin{cases} \lambda_w \dfrac{w_{i,\min} - w_i}{w_{i,\min}}, & w_i < w_{i,\min} \\ 0, & w_{i,\min} \leq w_i \leq w_{i,\max} \\ \lambda_w \dfrac{w_i - w_{i,\max}}{w_{i,\max}}, & w_i > w_{i,\max} \end{cases} \tag{33}$$

To ensure the feasibility of the optimization results, not only the constraints of heat sources but also the constraints of the heat supply network should be considered. The constraints of the urban heating network are mainly reflected in the transmission and distribution capacity of the network, that is, the hot water flow rate should be kept within a certain range. Where f_w is the velocity deviation coefficient of the pipe network. $f_{w,\max}$ is the maximum value of f_w. Δw_i is the deviation between the working fluid flow rate and the specified flow rate in a section. δ_{wi} is the maximum allowable deviation. λ_w is the penalty coefficient for flow rate deviation in heat supply quality calculation. w is the working fluid flow rate.

In addition, to avoid the hydraulic imbalance problem in the heating system, constraints of heating network distribution capacity should be considered. The key is to determine whether there is a solution satisfying the distribution capacity of the heating network under the combination of pumps, valves, and the heat load distribution. In this paper, through solving the heating network model mentioned above, if the flow rate and the pressure distribution are positive, the system achieves in matching supply and demand of heat sources and users. Otherwise, the given heat load distribution is invalid.

IV. PARTICLE SWARM OPTIMIZATION(PSO)

A. BASIC PRINCIPLES OF PARTICLE SWARM OPTIMIZATION

Particle swarm optimization is a typical swarm intelligence optimization algorithm. Its idea originates from the research and behavior simulation of the simplified social model of bird swarms [26].

In the process of particle swarm optimization, each particle flies at a certain speed in the n-dimensional search space. Suppose $X_i = (x_{i1}, x_{i2}, \ldots, x_{in})$ is the current position of particle i, $V_i = (v_{i1}, v_{i2}, \ldots, v_{in})$ is the current flying speed of particle i, $pbest_i = (pbest_{i1}, pbest_{i2}, \ldots, pbest_{in})$ is the optimal position experienced by particle i.

In the load scheduling optimization problem of multi-source district heating system, particles represent different load scheduling schemes, and the current position of particles represents the objective function value under the load allocation scheme. When the total heat load is constant, the dimension n of particles is related to the number of heat sources k, $n = k - 1$.

Assuming that the utility function $G(D)$ of multi-objective optimization of multi-source complementary heating system is the maximum objective function, then the optimal position of particle i is determined by the following equation:

$$pbest_i(t+1) = \begin{cases} pbest_i(t), & \text{If } G(D_i(t+1)) \leq G(pbest_i(t)) \\ D_i(t+1), & \text{If } G(D_i(t+1)) \geq G(pbest_i(t)) \end{cases} \tag{34}$$

The number of particles in the population is N, and the best position that all particles have experienced is $gbest(t)$, it is the global optimal position.

$$gbest(t) = \max\{G(pbest_1(t)), G(pbest_2(t)), \ldots, G(pbest_N(t))\} \tag{35}$$

The particle's flight speed, which is the load variation range and position of each heat source in the load scheduling scheme, can be dynamically adjusted according to individual flight experience and group flight experience. The update equation of velocity and position is as follows:

$$v_{ij}(t+1) = wv_{ij}(t) + c_1\left(pbest_{ij}(t) - x_{ij}(t)\right) + c_2\left(gbest_j(t) - x_{ij}(t)\right) \tag{36}$$

$$x_{ij}(t+1) = x_{ij}(t) + v_{ij}(t+1) \tag{37}$$

where i is the ith particle. j is the j-th dimension of the particle. $v_{ij}(t)$ is the j-$dimension$ flight speed of the particle i when it evolves to the t-th generation. w is the inertia weight. $x_{ij}(t)$ is the j-$dimensional$ vector of particle i when it evolves to the t-th generation. $pbest_{ij}(t)$ is the optimal position of the j-th dimensional individual of particle i when it evolves to the t-th generation. $gbest_j(t)$ is the j-$dimension$ component of the optimal position $gbest$ of the whole particle swarm when it evolves to the t-th generation. c_1 and c_2 are the acceleration factor (also known as 'learning factor').

In the particle swarm optimization algorithm, all particles will advance to the global optimal position. At the same time, the optimization of individual particles in the group can ensure that the particles are explored in multiple regions, which can prevent the algorithm from ending early and falling into local optimization.

B. IMPROVED PARTICLE SWARM OPTIMIZATION

The MOO problem proposed can be solved by PSO. When operating in practice, it is necessary to combine the solution

with the dynamic operating conditions of a specific system. Based on the dynamic-objective method(DOM) [46], this paper introduces a complex constraint handling mechanism in primary PSO so that the MOO function and corresponding solution strategy can be reconstructed to adapt the load distribution of MSDHS. Compared to traditional PSO, the improved PSO based on DOM transforms constraints to a new objective function, which is firstly solved through defining distance function $\Phi(D)$. Therefore, the optimization problem with p inequality constraints and q equality constraints is expressed by the following equation:

$$\max F(x), \quad s.t. \begin{cases} g_i(X) \geq 0, & i = 1, 2, \ldots, p \\ h_j(X) = 0, & j = 1, 2, \ldots, q \end{cases} \tag{38}$$

The distance function corresponding to the constraint conditions is as follows:

$$\Phi(X) = \sum_{i=1}^{p} \max\{0, g_i(X)\} + \sum_{j=1}^{q} \{0, |h_j(X)| - \varepsilon\} \tag{39}$$

where ε is an arbitrarily small positive number. In the optimization of the heating system, we can take $\varepsilon = 1$. During the execution of the optimization algorithm, the original optimization goal will become the new optimization goal.

$$\max(\Phi(X), F(X)) \tag{40}$$

If the particle is not in the feasible region, $\Phi(X)$ is taken as the optimization objective to make the particle close to the feasible region. Only when $\Phi(X) = 0$ or $\Phi(X) \leq \delta$, the optimization of $F(X)$ starts. δ is the allowable error of constraint, which is taken as 0.2 in this paper. When optimization $F(X)$ is started, if the particles leave the feasible region again, the optimization target returns to $\Phi(X)$ again.

In this way, particles prefer approaching to feasible region, for which solution efficiency is improved. The flow chart of the improved PSO is shown in Fig. 4.

1) PARTICLE SWARM OPTIMIZATION PARAMETER SETTINGS

The parameters of the particle swarm optimization include population size N, inertia weight w.acceleration factor c_1, c_2, maximum particle speed $v_{\max}$, and maximum number of iterations T.

1) The maximum particle speed $v_{\max}$: In order to prevent the particle velocity from being too large and exceeding the search space range, it is necessary to limit the particle velocity. The update speed of all particles should be within $[-v_{\max}, v_{\max}]$, and if the particle is out of range, let it be the boundary value. It has little effect on the final result. In this paper, $v_{\max} = 0.5$.
2) The inertia weight w: The setting of inertia weight has a great influence on the final result. Inertia weight w refers to the ability of a particle to maintain the previous state of motion. At present, the setting methods of inertia weight mainly include constant setting, linear adjustment, fuzzy adaptive, and random adjustment [24], [25]. Shi *et al.* suggested setting the inertia weight to 0.8 [47]. Because the fuzzy adaptive method needs a lot of experience in setting weights, it is difficult to apply in thermal engineering. In this paper, three schemes of setting fixed value, linear adjustment, and random adjustment are compared. The calculation equations of linear adjustment and random adjustment are as follows:

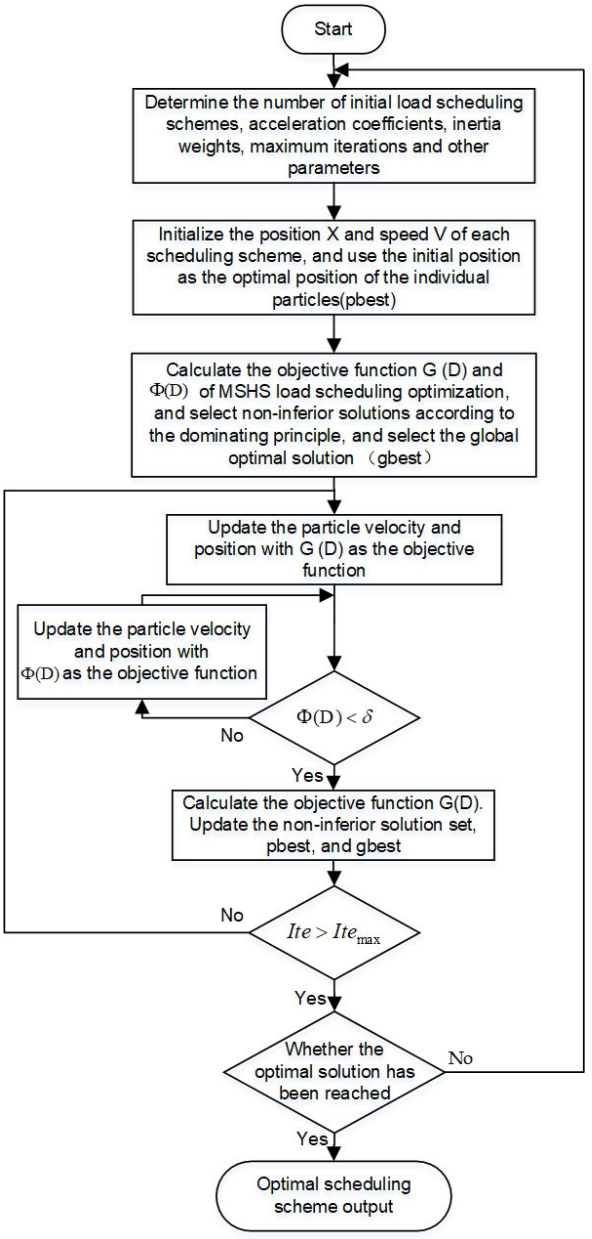

FIGURE 4. Flow chart of improved particle swarm multi-objective optimization algorithm based on DOM constraint mechanism.

$$w(t) = (w_1 - w_2)\frac{T - t}{T} + w_2 \tag{41}$$

$$w(t) = 0.5 + \frac{rand()}{2} \tag{42}$$

where w_1 and w_2 represents the initial value and terminal value of inertia weight respectively. T and t are the

maximum evolution algebra and the current evolution algebra respectively. *rand* () is a random number in the interval [0,1].

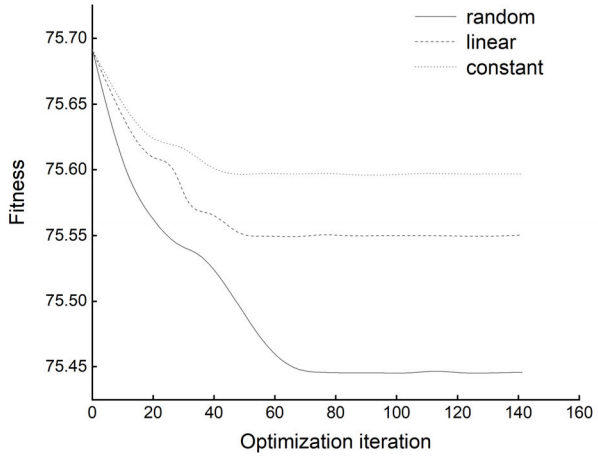

FIGURE 5. Influence of inertia weight setting on fitness.

The final result is shown in Fig. 5. It can be seen from the figure that when the inertia weight is set randomly, the algorithm achieves convergence around the 80th generation, and the final convergence accuracy is 75.45. In summary, the weight coefficient of random adjustment is better than the other two methods. For the problem of high precision, the randomly adjusted inertia weight ensures the diversity of particles to a certain extent. Therefore, this paper uses the weight coefficient set randomly.

3) The acceleration factor c_1, c_2: c_1 and c_2 respectively represent the acceleration weight of each particle moving towards the *pbest* and *gbest* directions. There are two kinds of acceleration factor setting strategies: constant setting and linear adjustment. Kennedy *et al* [26] suggested that setting the acceleration factor to two can achieve the best convergence results. Ratnaweera *et al* [28] thought that the linear adjustment was better than the constant setting. The equation of linear adjustment is:

$$c_1(t) = (c_{1f} - c_{1i})\frac{T-t}{T} + c_{1i} \tag{43}$$

$$c_2(t) = (c_{2f} - c_{2i})\frac{T-t}{T} + c_{2i} \tag{44}$$

where c_{1i}, c_{2i} is the initial value of c_1 and c_2 respectively. c_{1f}, c_{2f} is the final value of c_1 and c_2 respectively. T and t are the maximum evolution algebra and the current evolution algebra respectively.

As can be seen from Fig. 6, there is little difference between the optimization accuracy of the two methods, but the optimization iterations of the constant setting are few. This paper takes $c_1 = c_2 = 2$.

4) The maximum number of iterations T: The maximum number of iterations of the algorithm is the termination

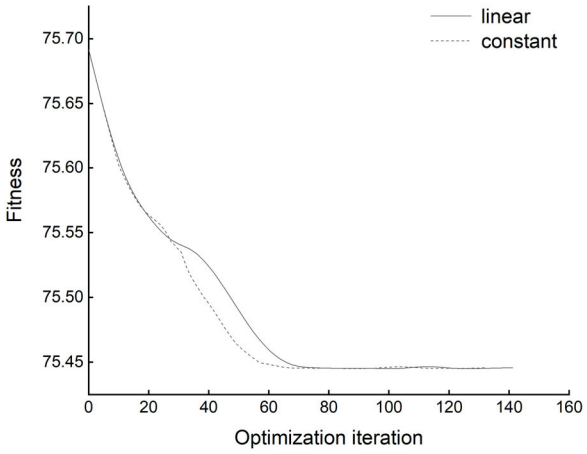

FIGURE 6. Influence of acceleration factor setting on fitness.

condition of the algorithm, and its value should be determined according to the specific situation. In this paper, $T = 200$.

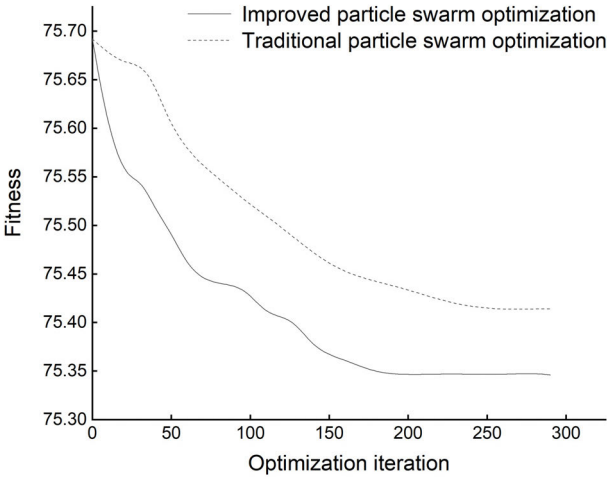

FIGURE 7. Influence of improved particle swarm optimization on fitness.

It can be seen from Fig. 7 that compared with the traditional particle swarm optimization, the improved PSO has faster convergence speed and better convergence accuracy.

This paper adopted the scheme of real coding.The mechanism model of this study was implemented in C++ programming language, and the optimization algorithm was implemented in Python.

V. CASE STUDY AND RESULTS ANALYSIS

A. INTRODUCTION TO THE PILOT HEATING SYSTEM

After establishing the mechanism model and optimization scheduling model above, this paper selected a central heating system in a certain city in China as the experimental and verification site. The composition of heat sources in this city's heating system is diverse, and the structure of the heat supply network is complex. There are three central heat sources in

the heating system. Among them, the combined design heat capacity of the #1 and #2 CHP units is about 370-380MW; the #3 and #4 CHP units are designed to provide 620MW heat capacity. Another heat source is four 116MW gas-fired hot water boilers, which are connected to the main network for commissioning operation during the heating season. The different capacities of heat sources lead to different efficiencies, which gives room to load distribution optimization.

FIGURE 8. Schematic diagram of heating network in the heating area.

At present, there are 230 heating stations in the heating area. The overall heating area is divided into two main network lines, which are shown in Fig. 8. Heat source A has two cogeneration units, which are called #1 and #2 CHP units. Mainline E (blue part in Fig. 8) has a heating area of 8.5 million m^2, which is supplied by the #1 and #2 CHP units. Heat source B also has two cogeneration units, which are called #3 and #4 CHP units. Mainline D (red part in Fig. 8) has a heating area of seven million m^2, which is mainly supplied by the #3 and #4 CHP units. Heat source C has four gas-fired boilers. It's an auxiliary heat source.

During the operation MSDHS, the heat demand is provided by each heating station based on the heating area and weather data over the years. These heat demands are accumulated and sent to the heat sources. For example, Fig. 9 is the heat load distribution map recorded in mainline E in one month. As can be seen, the daily load varies in a relatively narrow scope. Once the heat demand from all lines (main line, sublines) are accumulated, the overall heat demand accepted by the heat sources is flattened. In this study, the typical day was selected from the load-interval with the highest amount of days.

B. MODEL VALIDATION

The centralized control room of the thermal power plant is equipped with a distributed control system (DCS), through which the operation data acquisition of the whole power plant can be realized. The accuracy of the simulation data is checked by comparing the data recorded in DCS under different load conditions with the theoretical model simulation results in Section 2.

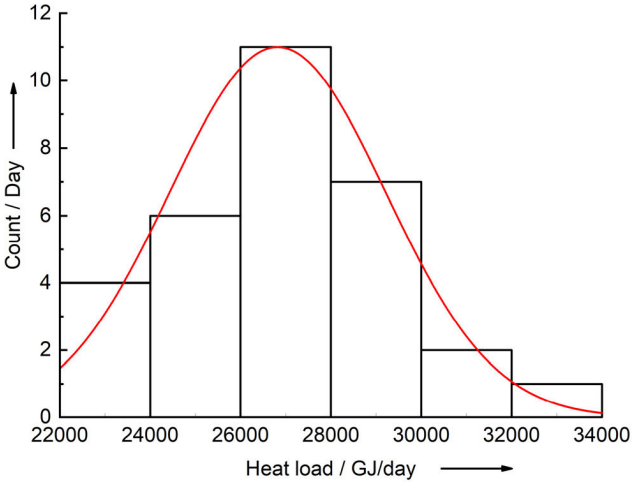

FIGURE 9. Heat load distribution map of mainline A in December 2017.

Table 3 and Table 4 show the heat load, power generation, and coal consumption for heating of #1, #2 and #3, #4 thermal power plants respectively from DCS. Table 5 shows the gas consumption of four gas-fired boilers under different heat load demands.

TABLE 3. The operation data of #1 and #2 CHP units.

Heat load (GJ/h)	Power generation (MW)	Coal consumption (t/h)
900.61	171.29	37.70
900.86	171.27	37.71
971.53	167.95	40.13
972.97	167.86	40.17
1045.69	164.61	42.51
1046.34	164.58	42.53
1115.08	161.27	44.85
1116.54	161.16	44.90
1187.60	157.93	47.31
1187.71	157.86	47.34
1260.32	154.59	49.76
1260.43	154.57	49.78
1331.24	149.59	52.14
1332.79	149.55	52.19

Fig. 10 and Fig. 11 show the relationship between fuel consumption and heat load of #1 and #2, #3 and #4 CHP units, respectively. The curve in the figure is the result of the theoretical model simulation in Section 2, and the scatter point is the actual operation data collected from DCS. It can be seen from the figure that the simulation results are in good agreement with the actual operation data, and the determination coefficients R^2 are all greater than 0.95, indicating that the simulation results have high reliability.

It can be seen from the figure that the simulation results are in good agreement with the actual operation data, and the determination coefficients R^2 are all greater than 0.95, indicating that the simulation results have high reliability.

TABLE 4. The operation data of #3 and #4 CHP units.

Heat load (GJ/h)	Power generation (MW)	Coal consumption (t/h)
1511.60	200.36	62.49
1513.41	200.34	62.56
1622.27	197.02	65.60
1623.17	196.93	65.64
1727.82	193.68	68.84
1729.12	193.65	68.89
1834.06	190.34	72.12
1834.67	190.23	72.14
1945.19	187.03	75.57
1945.48	186.94	75.58
2051.60	183.76	79.13
2054.34	183.63	79.24
2161.04	178.66	82.68
2162.59	178.59	82.72

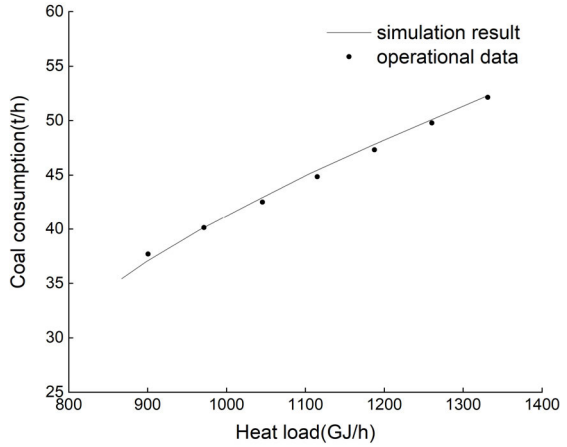

FIGURE 10. Curve of coal consumption with heat load of #1 and #2 CHP units.

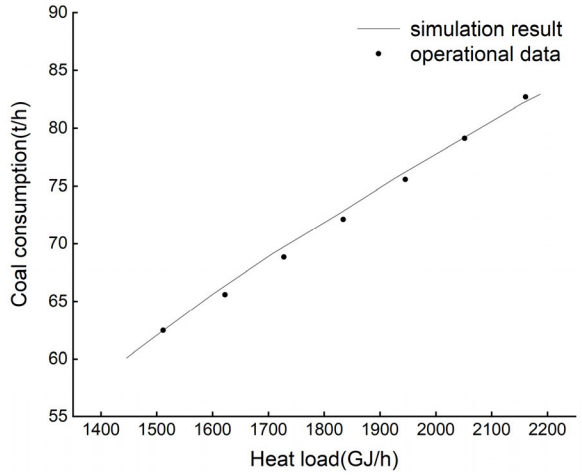

FIGURE 11. Curve of coal consumption with heat load of #3 and #4 CHP units.

It can be seen from Fig. 12 that although the configuration of the four gas-fired boilers is the same, the characteristic curves of the four units are different due to the aging of components during operation. Therefore, for a given load of the whole plant, it is necessary to optimize the load distribution among the heat sources and within the four gas-fired boilers.

TABLE 5. The operation data of 4 gas-fired boilers.

(Heat load	Fuel consumption of gas-fired boiler(Nm^3/h)			
(GJ/h)	1#	2#	3#	4#
229.68	6743.26	6645.26	6702.26	6657.26
250.56	7359.76	7280.76	7338.76	7289.76
271.44	7976.94	7920.94	7927.94	7909.94
292.32	8594.85	8557.85	8604.85	8538.85
313.20	9213.81	9199.47	9242.47	9172.47
334.08	9832.81	9836.81	9879.81	9803.81
354.96	10452.90	10471.95	10515.93	10436.91
375.84	11073.72	11110.79	11155.75	11078.77
396.72	11695.23	11757.28	11789.20	11721.26
417.60	12317.41	12390.42	12423.44	12364.48

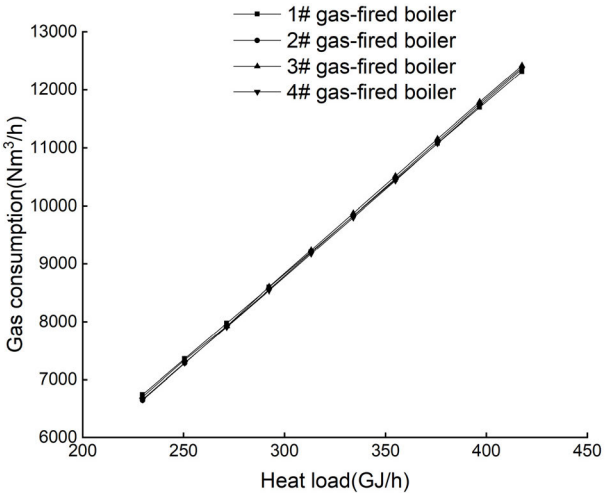

FIGURE 12. Curve of fuel consumption versus heat load of 4 gas-fired boilers.

C. OPTIMIZATION VALIDITY TEST

In order to illustrate the validity of optimization, this study selected the working conditions of one day in December 2017 for comparison.

By applying the PSO method, the process curve of the MSDHS utility function is shown in Fig. 13. The utility function expresses the proximity of each load dispatch scheme to the optimal. It ends with the optimal scheme when the value of the utility function is close to one. To minimize optimization, the utility function value is taken as negative. After 100 optimization iterations, the value of the utility function stabilizes, which means that the algorithm has found the optimal solution, and the corresponding value is 0.818. The time complexity of the algorithm is analyzed objectively by the ''big-O notation'' [48]. The time complexity of the algorithm is $O(NTd)$, where N is the population size, T is the maximum number of iterations, d is the space dimension.

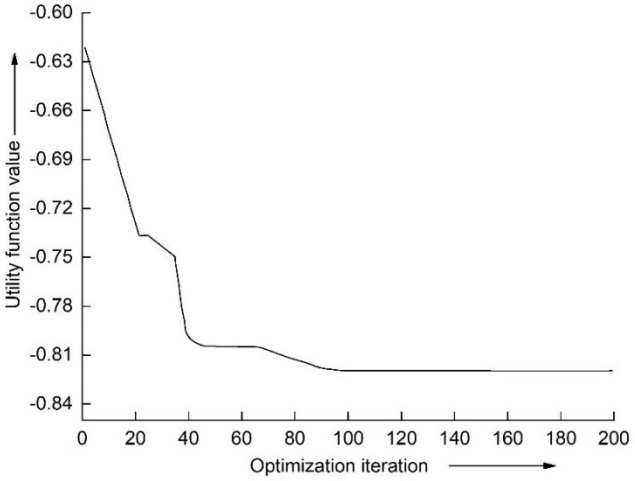

FIGURE 13. Process curve of PSO.①.

Each optimization time is less than five minutes, which can fully meet the engineering requirements compared with the thermal system once an hour.

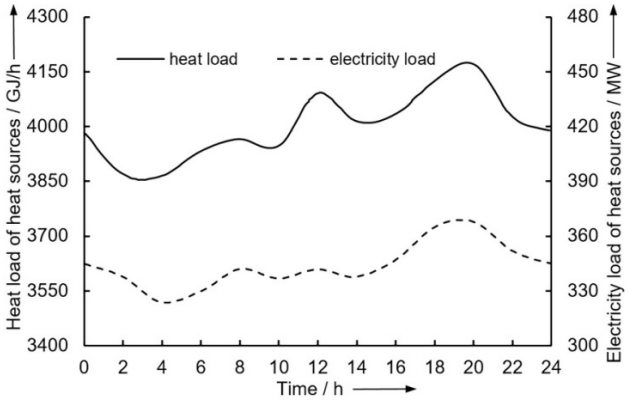

FIGURE 14. Diagram of the distribution of heat load and electricity load over time in the site.

Fig. 14 shows the overall heat and electricity load change curve of the day. PSO algorithm is also used to optimize the load distribution among different heat sources, and finally, the diagrams of heat source optimization comparison shown in Fig. 15, 16, and 17 can be obtained.

Fig. 15 shows the heat load change curve of each heat source over time. At 0-10 a.m., the gas-fired boilers are maintained in a constantly low load state, because the total heat load is low. Under this circumstance, the load of #1 and #2 CHP units is reduced to maintain the energy balance in the energy system.

In the periods from 11 a.m. to 1 p.m. and from 7 p.m. to 9 p.m., the total heat load increases, and the heat load is at the peak stage. During these two periods, the output of each heat source is increased to meet the need of heat load. Fig. 16 shows the percentage of each heat source's output after optimization. It can be seen that the heat load of the #3 and #4 CHP units is the highest, accounting for 46.1%, and

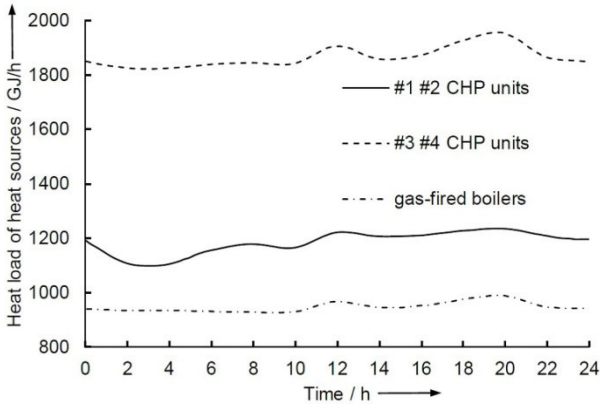

FIGURE 15. Diagram of the heat load of each heat source over time.

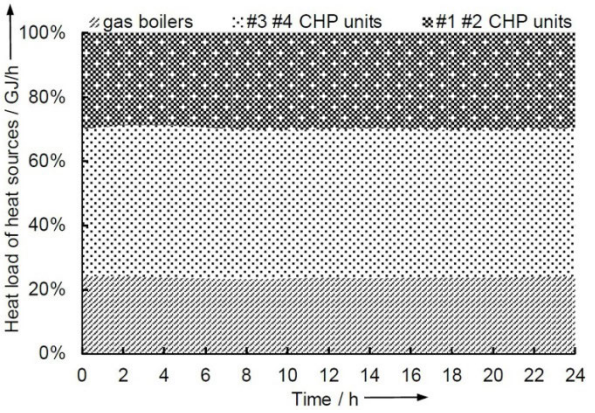

FIGURE 16. Diagram showing the distribution of the percentage of heat sources' output over time.

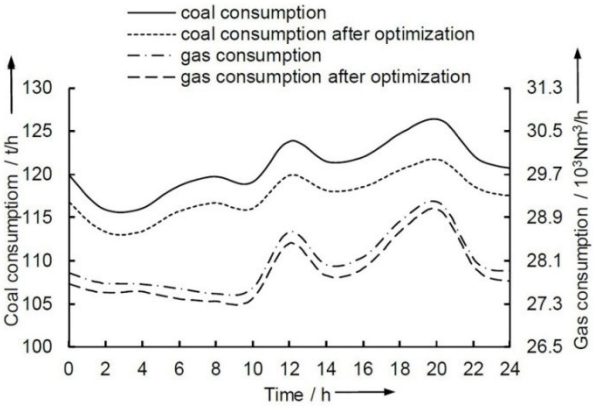

FIGURE 17. Diagram of fuel consumption change with time before and after optimization of MSDHS.

the heat load of the gas-fired boilers is the lowest, basically maintaining 23.8%. There are almost no fluctuations among the output of different heat sources.

Fig. 17 is a comparison of the total fuel consumption before and after optimization. It can be found that the fuel consumption of the optimized heating system is generally lower than that of the original empirical load distribution scheme.

The average fuel saving is 1.14%, and the gas-saving is 0.53%. By assuming the coal price of \$77/t and the gas price of \$0.35/m^3, this optimization method can save \$3,270 in the 24-hour project verification.

D. RESULTS ANALYSIS

In order to further show the feasibility and necessity of the optimization scheme, we calculate the load distribution results of each source under different total heat loads and further analyze the results.

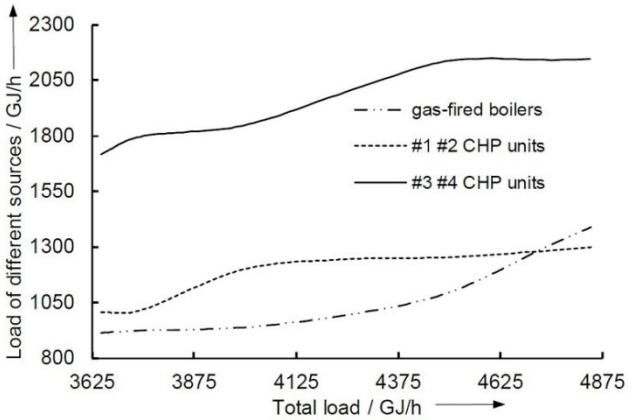

FIGURE 18. Curve of heat load distribution as a function of the total load.

After optimizing via PSO, the curves of heat load distribution among different heat sources changing with the total load are illustrated in Fig. 18. It shows that the heat load of #1 and #2 CHP units increases rapidly when the total heat load is low, which is 3750-4000 GJ/h. In the meantime, the load variation of #3 and #4 CHP units is smooth. In this case, considering that the three objective functions are related to the fuel consumption, increasing the heat load of #1 and #2 CHP units can make the whole heating system achieve better economic and environmental benefits while adding total load. When #1 and #2 CHP units are close to design load in the situation of the total load ranging from 4000 to 4500 GJ/h, it is sufficient to satisfy heat demand and meet the relatively optimal performance of the heating system by increasing heat load of #3 and #4 CHP units. As the total load increases to 4500-4750 GJ/h, increasing the heat load of the gas-fired boilers is the only method to meet the total heat demand because all CHP units have been near the design load.

It can be seen from Fig. 18 that when the total heat load increases, the two CHP units can achieve the maximal overall system efficiency. There are two reasons. On one hand, the weight of the economic index is high. On the other hand, the prices of fuel used by CHP units and gas-fired boilers are quite different, and the heating cost of gas-fired boilers is higher, which makes it costly to use gas-fired boilers. Therefore, the scheduling load of the CHP units in preference to the gas-fired boilers are a reasonable way to achieve optimal system economy.

In the heating system studied in this paper, due to the diversity of heat sources and the complexity of the heat supply network structure, after the optimal load dispatch among the three heat sources in the first level is determined, the load distribution of four gas-fired boilers is optimized, as shown in Fig. 19.

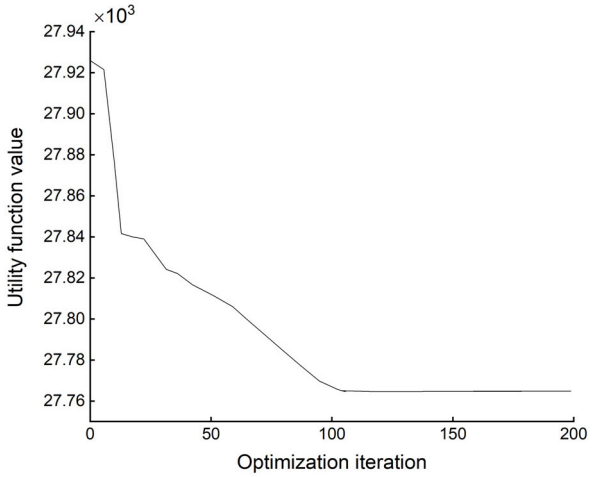

FIGURE 19. Process curve of PSO.②.

For the gas-fired boiler heating system, because it only uses a single fuel (natural gas), its energy consumption and environmental benefits are consistent, that is, under the condition of meeting a certain heat load, the less fuel used, the greater the economic benefits and the fewer pollutant emissions.

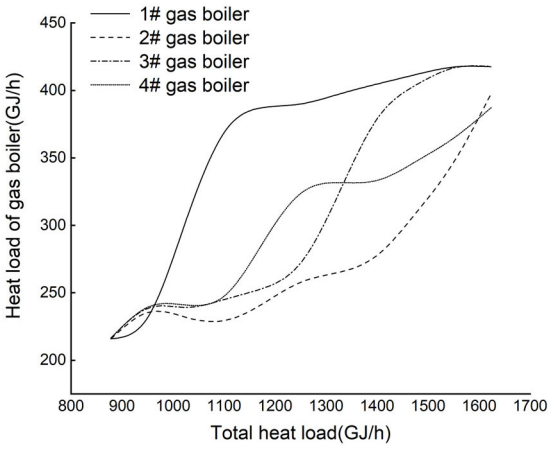

FIGURE 20. Load distribution variation diagram of 4 gas-fired boilers.

It can be seen from Fig. 19 that after 110 iterations, the curve tends to be stable, and the particle swarm optimization algorithm finds the relative optimal solution. Under this load scheduling scheme, the gas consumption is the least and the heating system is the most economical. Fig. 20 shows that when the total heat load of the gas boiler increases, increasing the load of one of the gas boilers to meet the overall heat load demand can maximize the economy of the entire heating

TABLE 6. Comparison of fuel consumption values before and after optimization under specific heat load.

Parameter		Heat load D_i (GJ/h)	Fuel consumption M_f or f (t/h | Nm^3/h)	Utility function value C_1	C_2	C_3
Original condition	#1 #2 CHP	1,235.4	49.7	0.371	0.092	0.184
	#3 #4 CHP	1,951.4	76.7			
	Gas boilers	988.9	29,168.0			
Optimal condition	#1 #2 CHP	1,297.4	50.7	0.467	0.116	0.232
	#3 #4 CHP	1,885.1	74.4			
	Gas boilers	993.2	29,047.0			

system. When the gas boiler is at a higher load Increasing the load of other gas-fired boilers can reduce the total fuel consumption, which is caused by the differences in the fuel consumption curves of the four gas-fired boilers.

Based on the optimal load distribution of heat sources, this study compares fuel consumption before and after optimizing distribution in an actual situation, where the total heat load is 4175 GJ/h. It can be seen from the above analysis that increasing the heat load of #1 and #2 CHP units helps to realize multi-objective comprehensive optimization. After optimizing working conditions in actual heating units, comparison data is shown in Table 6. As seen in Table 6, after optimization by improved particle swarm algorithm, the heat load of #1 and #2 CHP units increases, leading to a reduction of 1.34 t/h of coal consumption (1.06% of the total fuel usage). In terms of gas-fired boilers, through the optimal distribution of four gas-fired boilers, gas consumption decreases by 139 Nm^3/h (0.48% of the total fuel usage), while the heat load slightly increases. Compared with the original condition, the utility function value of each primary index under the optimized working condition has been improved, and the economic index has been improved the most. Therefore, it is of great significance to optimize the load scheduling of a multi-source complementary heating system through PSO.

There are two limits to this study. First, to facilitate the applicability of the proposed method in the real site, this study uses the weight method rather than more advanced methods to solve the MOO problem. Second, this study does not discuss the impact of the proposed approach when applied to an MSDHS with a greater covered area and more diverse heating sources (including renewable energy-based heating sources). Under that condition, the system uncertainty will increase. With the increase of population size, the convergence time of the algorithm may be longer and the convergence accuracy may be worse. Compared with other optimization algorithms, the improved particle swarm optimization proposed in this paper is slightly insufficient in dealing with the problem of local optimization. The future work followed by this study will focus on two aspects. First, the future work will demonstrate this method in a larger MSDHS (covering an area of 100 million m^2) with more uncertainties. We plan to report the impact of this methodology in a scaled-up megacity and discuss the challenges introduced by the scale of the system after a complete run in heating season. The second is the comparison between the proposed method and conventional gradient-based methods from both simulation and field test aspects while introducing regional particulate matter data into the objective functions. This shall also include the enhancement of the MOO process by generating its Pareto front.

VI. CONCLUSION

After considering the influence of the heating network on the feasibility of dispatching strategies, this paper firstly gives a real-time optimization model of load scheduling for MSDHS. Secondly, from the three perspectives of economy, energy structure, and environment, this paper establishes a multi-objective optimization evaluation system for MSDHS where FAHP analysis is used to find out the corresponding weight factors of each objective function to formulate an integrated objective function. Thirdly, this paper solves the optimal load distribution strategy of multiple heat sources with the improved PSO algorithm. Finally, this paper takes a real MSDHS and its covered heating area as a pilot site. The above optimization scheme is verified by the example of the load distribution in each heat source of the site. The results show that the optimized load scheduling scheme can make the comprehensive utility function value of the heating system higher. By optimizing the daily heat load in the pilot site, the total coal consumption can be saved by about 1.14%, the gas consumption can be saved by about 0.53%, and the cost can be saved by more than $3,270, justifying the economic feasibility of the study.

REFERENCES

[1] *China Energy Statistical Yearbook*, National Bureau of Statistics of China, Beijing, China, 2010. [Online]. Available: https://data.cnki.net/area/Yearbook/Single/N2008070077?z=D20
[2] *Building Energy Conservation Research Center of Tsinghua University*, China Architecture & Building Press, Beijing, China, 2019, pp. 10–25.
[3] *China Energy Statistical Yearbook*, National Bureau of Statistics of China, Beijing, China, 2017. [Online]. Available: https://data.cnki.net/area/Yearbook/Single/N2008070077?z=D20
[4] W. Na, Y. Song, and D. Y. Li, "A hydraulic modeling of loop pipeline network with multiple heat sources based on graph theory," *Adv. Mater. Res.*, vol. 5, pp. 740–744, Dec. 2011, doi: 10.4028/www.scientific.net/AMR.374-377.740.
[5] L. Dingkai, "A mathematical modeling and algorithm for optimization of general district heating system," *J. Eng. Thermophys.*, no. 2, pp. 101–106, Feb. 1988.
[6] I. Gabrielaitiene, B. Bøhm, and B. Sunden, "Modelling temperature dynamics of a district heating system in naestved, Denmark—A case study," *Energy Convers. Manage.*, vol. 48, no. 1, pp. 78–86, Jan. 2007, doi: 10.1016/j.enconman.2006.05.011.
[7] W. Yang, F. Wen, K. Wang, Y. Huang, and M. Salam, "Modeling of a district heating system and optimal heat-power flow," *Energies*, vol. 11, no. 4, p. 929, Apr. 2018, doi: 10.3390/en11040929.
[8] L. Li, M. Zaheeruddin, S.-H. Cho, and S.-H. Jung, "Steady state and dynamic modeling of an indirect district heating system," *Int. J. Air-Conditioning Refrig.*, vol. 18, no. 01, pp. 61–75, Mar. 2010, doi: 10.1142/S2010132510000083.

[9] S.-Y. Choi, K.-Y. Yoo, J.-B. Lee, C. B. Shin, and M.-J. Park, "Mathematical modeling and control of thermal plant in the district heating system of korea," *Appl. Thermal Eng.*, vol. 30, nos. 14–15, pp. 2067–2072, Oct. 2010, doi: 10.1016/j.applthermaleng.2010.05.014.

[10] M. Karlsson, A. Gebremedhin, S. Klugman, D. Henning, and B. Moshfegh, "Regional energy system optimization – potential for a regional heat market," *Appl. Energy*, vol. 86, no. 4, pp. 441–451, Apr. 2009, doi: 10.1016/j.apenergy.2008.09.012.

[11] B. Zhang, "Taiyuan the operation condition of the heat source system analysis and determine the best solution," M.S. thesis, Dept. Arch., BCEA Univ., Beijing, China, 2016. [Online]. Available: https://kns.cnki.net/kcms/detail/detail.aspx?FileName=1017028545.nh&DbName=CMFD2017

[12] E. Bowitz and M. D. Trong, "The social cost of district heating in a sparsely populated country," *Energy Policy*, vol. 29, no. 13, pp. 1163–1173, 2001, doi: 10.1016/S0301-4215(01)00039-8.

[13] X. Er, "Assessing and optimizing the economic and environmental impacts of distributed power generation," *J. Eng. Thermophys.*, vol. 25, no. 2, pp. 189–192, 2004. [Online]. Available: https://kns.cnki.net/kcms/detail/detail.aspx?FileName=GCRB200402002&DbName=CJFQ2004

[14] P. J. Agrell and P. Bogetoft, "Economic and environmental efficiency of district heating plants," *Energy Policy*, vol. 33, no. 10, pp. 1351–1362, Jul. 2005, doi: 10.1016/j.enpol.2003.12.011.

[15] R. P. Hamalainen and J. Mantysaari, "Dynamic multi-objective heating optimization," *Eur. J. Oper. Res.*, vol. 142, no. 1, pp. 1–15, Dec. 2002, doi: 10.1016/S0377-2217(01)00282-X.

[16] C. Juexian, "Application of grey system theory to select optimum heating model," *J. Shenyang Inst. Eng.*, vol. 3, no. 3, pp. 234–236, 2007. [Online]. Available: https://kns.cnki.net/kcms/detail/detail.aspx?Filename=SYDL200703009&Dbname=CJFQ2007

[17] W. Liu and H. Ang, "Study on comprehensive evaluation model of thermal system," *J. Eng. Therm. Energy Power*, vol. 18, no. 3, pp. 233–236+321-322, 2003. [Online]. Available: https://kns.cnki.net/kcms/detail/detail.aspx?FileName=RNWS200303004&DbName=CJFQ2003

[18] Y. Zhang and M. Ding, "Application of fuzzy mathematics to comprehensive evaluation of the heating system," *J. Lanzhou Jiaotong Univ.*, vol. 26, no. 3, pp. 38–40, 2007. [Online]. Available: https://kns.cnki.net/kcms/detail/detail.aspxFileName=LZTX200703010&DbName=CJFQ2007

[19] X. He and J. Sheng, "New evaluation system for the modernization level of a province or a city based on an improved entropy method," *Environ. Monitor. Assessment*, vol. 192, no. 1, pp. 1–10, Jan. 2020, doi: 10.1007/s10661-019-7904-3.

[20] M. Sepehri, H. Malekinezhad, S. Z. Hosseini, and A. R. Ildoromi, "Assessment of flood hazard mapping in urban areas using entropy weighting method: A case study in hamadan city, iran," *Acta Geophys.*, vol. 67, no. 5, pp. 1435–1449, Oct. 2019, doi: 10.1007/s11600-019-00342-x.

[21] X. Wei, H. Chang, B. Feng, Z. Liu, and C. Huang, "Hull form reliability-based robust design optimization combining polynomial chaos expansion and maximum entropy method," *Appl. Ocean Res.*, vol. 90, Sep. 2019, Art. no. 101860, doi: 10.1016/j.apor.2019.101860.

[22] T. L. Saaty, "How to make a decision: The analytic hierarchy process," *Eur. J. Oper. Res.*, vol. 48, no. 1, pp. 9–26, Sep. 1990, doi: 10.1016/0377-2217(90)90057-I.

[23] O. S. Vaidya and S. Kumar, "Analytic hierarchy process: An overview of applications," *Eur. J. Oper. Res.*, vol. 169, no. 1, pp. 1–29, Feb. 2006, doi: 10.1016/j.ejor.2004.04.028.

[24] X. Guo, M. Ji, Z. Zhao, D. Wen, and W. Zhang, "Global path planning and multi-objective path control for unmanned surface vehicle based on modified particle swarm optimization (PSO) algorithm," *Ocean Eng.*, vol. 216, Nov. 2020, Art. no. 107693, doi: 10.1016/j.oceaneng.2020.107693.

[25] R. S. Beed, A. Roy, S. Sarkar, and D. Bhattacharya, "A hybrid multi?objective tour route optimization algorithm based on particle swarm optimization and artificial bee colony optimization," in *Proc. Comput. Intell.*, Bangkok, Thailand, 2020, pp. 884–909, doi: 10.1111/coin.12276.

[26] J. . Kennedy and R. C. Eberhart, "Particle swarm optimization," in *Proc. Int. Conf. Netw.*, 2002, vol. 4, no. 1, pp. 1942–1948, doi: 10.1109/ICNN.1995.488968.

[27] A. Chatterjee and P. Siarry, "Nonlinear inertia weight variation for dynamic adaptation in particle swarm optimization," *Comput. Oper. Res.*, vol. 33, no. 3, pp. 859–871, Mar. 2006, doi: 10.1016/j.cor.2004.08.012.

[28] A. Ratnaweera, S. K. Halgamuge, and H. C. Watson, "Self-organizing hierarchical particle swarm optimizer with time-varying acceleration coefficients," *IEEE Trans. Evol. Comput.*, vol. 8, no. 3, pp. 240–255, Jun. 2004, doi: 10.1109/TEVC.2004.826071.

[29] D. Sedighizadeh, E. Masehian, M. Sedighizadeh, and H. Akbaripour, "GEPSO: A new generalized particle swarm optimization algorithm," *Math. Comput. Simul.*, vol. 179, pp. 194–212, Jan. 2021, doi: 10.1016/j.matcom.2020.08.013.

[30] I. C. Trelea, "The particle swarm optimization algorithm: Convergence analysis and parameter selection," *Inf. Process. Lett.*, vol. 85, no. 6, pp. 317–325, 2003, doi: 10.1016/S0020-0190(02)00447-7.

[31] J. J. Liang, A. K. Qin, P. N. Suganthan, and S. Baskar, "Comprehensive learning particle swarm optimizer for global optimization of multimodal functions," *IEEE Trans. Evol. Comput.*, vol. 10, no. 3, pp. 281–295, Jun. 2006, doi: 10.1109/TEVC.2005.857610.

[32] O. Le Corre, G. Brecq, and M. Tazerout, "Thermoeconomic analysis based on energy structure for combined heat and power," *Appl. Therm. Eng.*, vol. 22, no. 5, pp. 561–566, 2002, doi: 10.1016/S1359-4311(01)00099-0.

[33] Y. F. Wang, M. X. Wang, Y. Liu, L. Yin, X. R. Zhou, J. F. Xu, and X. Y. Zhang, "Fuzzy modeling of boiler efficiency in power plants," *Inf. Sci.*, vol. 542, pp. 391–405, Jan. 2021, doi: 10.1016/j.ins.2020.06.064.

[34] H. Cai, C. Ziras, S. You, R. Li, K. Honoré, and H. W. Bindner, "Demand side management in urban district heating networks," *Appl. Energy*, vol. 230, pp. 506–518, Nov. 2018, doi: 10.1016/j.apenergy.2018.08.105.

[35] M. Zhe, "Discussion and Countermeasures of Current Situation of Central Heating in Our Country," *J. East China Jiaotong Univ.*, vol. 23, no. 3, pp. 66–69, 2004. [Onine]. Available:. [Online]. Available: https://kns.cnki.net/kcms/detail/detail.aspx?FileName=HDJT200403018&DbName=CJFQ2004

[36] J. Liu and L. Xu, "Load assignment strategy for natural gas-fired boilers in Tsinghua University," *J. Tsinghua Univ.*, vol. 43, no. 12, pp. 1657–1660, 2003, doi: 10.16511/j.cnki.qhdxxb.2003.12.021.

[37] W. Zhong, H. Feng, X. Wang, D. Wu, M. Xue, and J. Wang, "Online hydraulic calculation and operation optimization of industrial steam heating networks considering heat dissipation in pipes," *Energy*, vol. 87, pp. 566–577, Jul. 2015, doi: 10.1016/j.energy.2015.05.024.

[38] Z. Xu, "An overview of methods for determining OWA weights," *Int. J. Intell. Syst.*, vol. 20, no. 8, pp. 843–865, Aug. 2005, doi: 10.1002/int.20097.

[39] M. G. Gong, "Research on evolutionary multi-objective optimization algorithms," *J. Softw.*, vol. 20, no. 20, pp. 271–289, 2009. [Online]. Available: https://www.researchgate.net/publication/265584234_Research_on_Evolutionary_Multi-Objective_Optimization_Algorithms, doi: 10.3724/SP.J.1001.2009.03483.

[40] S. Liu, J. Forrest, and Y. Yang, "A brief introduction to grey systems theory," in *Proc. Int. Conf. Grey Syst. Intell. Services*, Beijing, China, 2011, vol. 2, no. 2, pp. 1–9, doi: 10.1109/GSIS35561.2015.

[41] W. Jiang-Jiang, Z. Chun-Fa, and J. You-Yin, "Multi-criteria analysis of combined cooling, heating and power systems in different climate zones in China," *Appl. Energy*, vol. 87, no. 4, pp. 1247–1259, Apr. 2010, doi: 10.1016/j.apenergy.2009.06.027.

[42] G. Xu, Y.-P. Yang, S.-Y. Lu, L. Li, and X. Song, "Comprehensive evaluation of coal-fired power plants based on grey relational analysis and analytic hierarchy process," *Energy Policy*, vol. 39, no. 5, pp. 2343–2351, May 2011, doi: 10.1016/j.enpol.2011.01.054.

[43] T. Tanino, "Fuzzy preference orderings in group decision making," *Fuzzy Sets Syst.*, vol. 12, no. 2, pp. 117–131, 1984, doi: 10.1016/0165-0114(84)90032-0.

[44] Y. Lu, "Weight calculation method of fuzzy analytical hierarchy process," *Fuzzy Syst. Math.*, vol. 16, no. 2, pp. 79–85, Jan. 2002. [Online]. Available: https://kns.cnki.net/kcms/detail/detail.aspx?FileName=MUTE200202013&DbName=CJFQ2002

[45] X. Li, Y. Han, and Z. Zhao, "The selection of heating method in residence zone," *Build. Energy Environ.*, vol. 403, no. 2, pp. 18–21, 2000. [Online]. Available: https://kns.cnki.net/kcms/detail/detail.aspx?FileName=JZRK200002006&DbName=CJFQ2000

[46] H. Lu and W. Chen, "Dynamic-objective particle swarm optimization for constrained optimization problems," *J. Combinat. Optim.*, vol. 12, no. 4, pp. 409–419, Oct. 2006, doi: 10.1007/s10878-006-9004-x.

[47] Y. Shi and R. Eberhart, "A modified particle swarm optimizer," in *Proc. IEEE Int. Conf. Evol. Comput.*, New York, NY, USA, 1998, pp. 69–73, doi: 10.1109/ICEC.1998.699146.

[48] S. Bae, *Big-O Notation BT—JavaScript Data Structures and Algorithms: An Introduction to Understanding and Implementing Core Data Structure and Algorithm Fundamentals*. Berkeley, CA, USA: Apress, 2019, pp. 1–11, doi: 10.1007/978-1-4842-3988-9_1.
[49] Y. Li, J. Wang, D. Zhao, G. Li, and C. Chen, "A two-stage approach for combined heat and power economic emission dispatch: Combining multi-objective optimization with integrated decision making," *Energy*, vol. 162, pp. 237–254, Nov. 2018, doi: 10.1016/j.energy.2018.07.200.

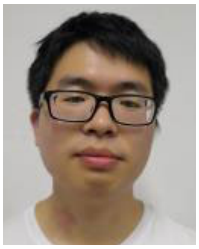

HAORAN ZHANG is currently pursuing the master's degree with the College of Energy Engineering, Zhejiang University. He is mainly engaged in modeling and simulation research of district heating system and the dynamic characteristics analysis of integrated energy system. He has been in charge of the modeling and analysis of several heating systems that span across both residential and industrial areas. He is currently working on the modeling and operation optimization of Shanghai chemical industrial park steam supply network, which is one of the largest industrial park energy systems in China.

DONGNIAN YIN is currently an Engineer of Wuxi Huilian Thermal Power Company Ltd. He is mainly engaged in the optimization of multi-unit heating load distribution. He has participated in a series of demonstration projects of intelligent interconnected industrial steam heat supply network in Jiangsu Province and the design of an intelligent monitoring scheme for large-scale multi-source district heating systems. He also works to develop the hydraulic balance algorithm and simulation system for the secondary network in district heating systems.

XIAOJIE LIN received the B.S. degree from Zhejiang University, in 2012, and the Ph.D. degree in mechanical engineering from the University of Maryland, College Park, in 2017. His Ph.D. advisors were Dr. Reinhard Radermacher and Dr. Yunho Hwang. After graduation, he worked with Mitsubishi Electric Research Laboratories, Boston, before joining the College of Energy Engineering, Zhejiang University, and later the Changzhou Industrial Technology Research Institute. He is currently a Postdoctoral Researcher with Zhejiang University, where he is also a Research Fellow with the Changzhou Industrial Technology Research Institute. He was working on variable refrigerant flow systems at the Center for Environmental Energy Engineering, University of Maryland. His research focuses on the optimal design and simulation of the multi-carrier complementary smart energy system with a special interest in urban and industrial heating. He has been working on the optimization and flexibility analysis of the energy system, since 2017. He is also interested in the potential of applying artificial intelligence to operation, design, and assessment of urban distributed energy systems.

RONG LIU is currently a Senior Engineer with Beijing Heating Group Company Ltd. She is mainly engaged in the field of energy and power engineering planning, heating system dispatch, and complex fluid network system analysis. She has participated in several joint international research projects focusing on smart heating technologies. Recently, she has been in charge of a Sino-Finnish government research project sponsored working on the development of a hydraulic balance algorithm for secondary network and the coordination dispatching between heating sources, network, substations, buildings, and users.

WEI ZHONG is currently a Professor with Zhejiang University. He is currently the Deputy Director of the College of Energy Engineering, Thermal Power Institute. He is mainly engaged in theoretical and technical research on the interdisciplinary fields between thermal power engineering and information technology. His research interests include intelligent energy system engineering, modeling of the complex multi-carrier energy systems, thermal system engineering, cyber-physics systems, and model predictive control. He is quite interested in various heating systems, including district heating and industrial heating systems and has published more than 30 academic articles in the area of heating system modeling.

CAISHAN CAO is currently a Senior Engineer with Linglong Group Company Ltd. He is mainly engaged in flexibility analysis of the heating system and has participated in the operation optimization of the heating sources including combined heat and power units. He is familiar with the technical economy of smart heating and is proficient in project development process management. He has more than 20 years of district heating system management and industrial heating system renovation experience.